J Forensic Sci, July 2006, Vol. 51, No. 4
doi:10.1111/j.1556-4029.2006.00182.x
Available online at: www.blackwell-synergy.com

TECHNICAL NOTE

Elias J. Kontanis,[1] *Ph.D., and Floyd A. Reed,*[2] *Ph.D.*

Evaluation of Real-Time PCR Amplification Efficiencies to Detect PCR Inhibitors

ABSTRACT: Real-time PCR analysis is a sensitive template DNA quantitation strategy that has recently gained considerable attention in the forensic community. However, the utility of real-time PCR methods extends beyond quantitation and allows for simultaneous evaluation of template DNA extraction quality. This study presents a computational method that allows analysts to identify problematic samples with statistical reliability by comparing the amplification efficiencies of unknown template DNA samples with clean standards. In this study, assays with varying concentrations of tannic acid are used to evaluate and adjust sample-specific amplification efficiency calculation methods in order to optimize their inhibitor detection capabilities. Kinetic outlier detection and prediction boundaries are calculated to identify amplification efficiency outliers. Sample-specific amplification efficiencies calculated over a four-cycle interval starting at the threshold cycle can be used to detect reliably the presence of 0.4 ng of tannic acid in a 25 μL PCR reaction. This approach provides analysts with a precise measure of inhibition severity when template samples are compromised. Early detection of problematic samples allows analysts the opportunity to consider inhibitor mitigation strategies prior to genotype or DNA sequence analysis, thereby facilitating sample processing in high-throughput forensic operations.

KEYWORDS: forensic science, real-time PCR, amplification efficiency, inhibitor detection, tannic acid, ancient DNA

Biological materials submitted for forensic DNA analysis are often compromised as a result of degradative processes and/or the presence of amplification inhibitors. When template DNA concentrations are below an optimal range, stochastic fluctuations can result in unequal sampling of heterozygous loci, leading to the false inference of a homozygous genotype, or cause nucleotide misincorporation during DNA sequencing (1–3). The presence of co-extracted PCR inhibitors can also confound template amplification and analysis (4,5). Severe inhibition will lead to the loss of alleles from the larger STR loci, or even complete false-negative results, whereas a slight to moderate inhibition can result in an underestimation of the affected sample's DNA concentration. This has potential consequences for downstream applications such as STR analysis, where adding too much template DNA can cause off-scale electrophoresis peaks. It is therefore advantageous to evaluate template DNA quantity and quality prior to genotyping or mtDNA sequencing so that samples can possibly be re-purified. While a variety of methods have been developed to quantitate template DNA before genotype or sequence analysis (6–9), none allow for simultaneous appraisal of template quantity and quality without the addition of an internal positive control that is co-amplified with the locus of interest. The primary objective of this study is to demonstrate empirically that along with template DNA quantitation, calculating real-time PCR amplification efficiencies can be used to identify samples contaminated by PCR inhibitors.

The development of real-time PCR quantitation methods coincides with advances in fluorescence-based detection assays (10,11). The primary advantages of real-time PCR quantitation include a wide dynamic range and high-throughput capabilities (6,12–14). Current detection platforms are able to detect less than 10 pg of DNA and process up to 384 samples (excluding quantitation standards and controls) in under 2 h. In addition, real-time PCR enables target-specific quantitation, allowing for sex determination (12,13,15), species identification (16), pathological diagnosis (17), and, with limited success, age prediction (18).

Real-time PCR template DNA quantitation estimates are derived from measured fluorescence accumulation, which is directly correlated to the amount of amplicon produced as the reaction progresses (19). Fluorescence signals are generated either by intercalating dyes that are specific for double-stranded DNA (20,21) or by sequence-specific oligonucleotide probes (22–24). The real-time PCR sequence detection system measures the reporter signal (R) and normalizes to a passive reference dye. Normalizing accounts for minor well-to-well variations in signal strength, allowing for more accurate sample-to-sample comparisons. The progressive cleavage of probe at each PCR cycle leads to an increase in normalized reporter signal (R_n) that is proportional to the initial number of template DNA molecules. However, during the initial PCR cycles, reporter fluorescence values are below the baseline detection capabilities of current real-time PCR systems, resulting in stochastic fluctuations in fluorescence (i.e. background fluorescence). To minimize this stochastic effect, normalized reporter signal is subtracted from background noise in the fluorescence signal. Normalized reporter signal minus the background fluorescence signal (ΔR_n) is then plotted against cycle number (Fig. 1*a*).

The real-time PCR fluorescence curve generated by the sequence detection system is composed of four distinct phases (Fig. 1*a*). When PCR product and reporter signal accumulates beyond background fluorescence levels, the reaction enters the exponen-

[1]Department of Ecology and Evolutionary Biology, Cornell University, Ithaca NY 14853.
[2]Department of Biology, University of Maryland, College Park, MD 20742.

Received 18 Sept. 2004; and in revised form 19 Oct. 2005 and 14 Feb. 2006; accepted 26 March 2006; published 23 June 2006.

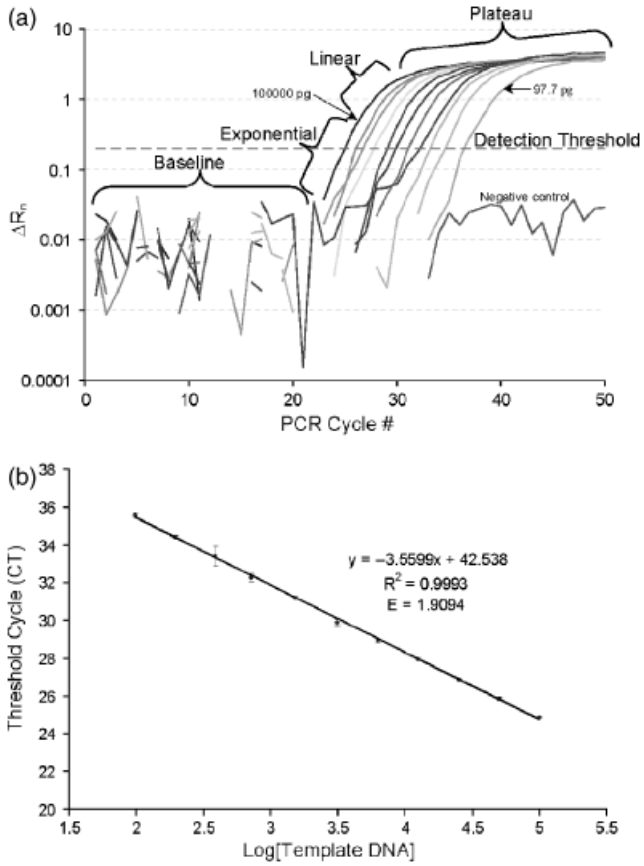

FIG. 1—*(a) Semi-log real-time amplification plot of a two-fold serial dilution series from 100,000 pg to 97.7 pg genomic DNA. (b) Quantitation standard curve of threshold cycle values plotted against the log of the initial template DNA concentration. Efficiency* $(E) = 10^{-1/slope}$.

tial detection phase. At this point, the amplification plot crosses a user-defined detection threshold that is set above the background fluorescence noise, preferably at the start of the exponential phase. The fractional cycle number at which the reaction crosses the threshold (CT) is inversely related to the initial template DNA concentration. As PCR product continues to accrue, the ratio of *Taq* DNA polymerase to amplicon decreases, resulting in non-exponential accumulation of product. At this point, the reaction enters the linear phase. Once PCR product ceases to accumulate due to assay depletion, ΔR_n values remain relatively constant and the reaction enters the plateau phase (Fig. 1*a*).

Quantitation is accomplished using a standard curve generated from the CT values of template DNA standards diluted over several orders of magnitude (Fig. 1*b*). The CT values of the standards are plotted against the log of the template DNA concentration. Template DNA concentrations of the unknown samples are extrapolated from their CT values. The validity of the standard curve method is predicated on the assumption of equal amplification efficiencies between DNA samples used as quantitation standards and unknown test samples. Reactions with depressed efficiencies will cross CT later than expected, resulting in erroneous quantitation estimates (25). Amplification efficiencies can fluctuate as a function of non-optimal assay design, enzyme instability, or the presence of co-extracted amplification inhibitors (26). Therefore, calculating amplification efficiencies allows for early detection of non-optimal assay conditions and will facilitate troubleshooting problematic samples prior to genotype or sequence analysis.

The relationship between amplified PCR product quantity and initial template quantity can be expressed as

$$N_A = N_0(E)^{C_A}$$

where the number of amplicons synthesized at cycle A (N_A) depends on the initial number of template molecules (N_0), reaction efficiency (E), and the elapsed number of cycles (C_A) (27). This efficiency definition reflects the fraction of extra yield from the preceding cycle (i.e. the proportion between current and previous amplicon quantities). In theory, each PCR target is replicated once every cycle, resulting in a maximum amplification efficiency value of two.

Liu and Saint (28) (hereafter referred to as the Liu and Saint method) apply the real-time PCR kinetic equation to calculate sample-specific amplification efficiencies at two arbitrary points (A and B) along the exponential phase of the reaction:

$$\Delta R_{n,A} = \Delta R_{n,0}(E)^{C_A}$$
$$\Delta R_{n,B} = \Delta R_{n,0}(E)^{C_B}$$

where fluorescence values (ΔR_n) have replaced DNA template quantity values (N), as template quantity is proportional to reporter fluorescence. If the aforementioned equations are expressed as a ratio, they simplify to

$$E = \left(\frac{\Delta R_{n,A}}{\Delta R_{n,B}}\right)^{1/(C_A - C_B)}$$

This equation assumes that efficiencies remain constant between points A and B, which is unlikely (29). Therefore, calculated efficiency represents an average over the selected range of cycles.

Ramakers et al. (30) use an iterative algorithm to locate the exponential phase of the real-time amplification plot (i.e. window of linearity). Sample-specific efficiency estimates are based on regression analysis of four to six data points within the window of linearity that have the highest coefficients of determination and slope closest to the maximum. Amplification efficiency is then calculated from the slope of the corresponding linear regression line:

$$E = 10^{\text{slope}}$$

Ruijter and Ramakers (31) developed the LinRegPCR program, which automates identification of the exponential phase and the amplification efficiency calculation. However, the analyst must evaluate the window of linearity in order to identify and adjust suspect reactions.

The aforementioned amplification efficiency calculation methods were designed to compare standards and test samples to ensure that quantitation estimates are accurate. Accuracy is essential when quantification is the end-product, such as when quantifying clinically pertinent gene expression levels (32). In the forensic community, template DNA quantitation is not the ultimate concern; however, erroneous quantitation estimates may confound subsequent analysis due to the addition of inadequate or overly concentrated amounts of template DNA. Early detection of aberrant amplification efficiencies will facilitate sample processing by allowing analysts to troubleshoot problematic reactions at an early stage of analysis, conserving time, reagents, and finite DNA samples (6).

While the Liu and Saint and LinRegPCR methods emphasize the importance of choosing data points within the exponential phase, there are no selection criteria recommendations for the Liu

and Saint calculation, or instructions for adjusting the window of linearity created by the LinRegPCR software. In this study, we identify the most effective adjustments that minimize variance in the efficiency estimate, consequently optimizing inhibitor detection sensitivity. Empirical analysis focuses upon PCR assays containing varying concentrations of DNA template and tannic acid, a naturally occurring PCR inhibitor (33–35). The Liu and Saint and LinRegPCR methods are evaluated and adjusted to maximize the reliability of the amplification efficiency estimate so that problematic template DNA samples can be identified.

Materials and Methods

Template DNA and PCR Inhibitor Dilution Series

Porcine (*Sus scrofa*) genomic DNA was used as the test template. Stock DNA purchased from Novagen® (Madison, WI) was supplied in TE (10 mM Tris-HCl, pH 8.0, 1 mM EDTA) at a concentration of 260 μg/mL (0.26 μg/μL). The A260:A280 spectrophotometric absorption ratio for the stock sample was 1.94, suggesting that the DNA is free from contaminating protein (36). A twofold serial dilution series ranging from 100,000 pg/2.5 μL to 97.7 pg/2.5 μL was created using stock genomic DNA and TE as the dilutent.

Tannic acid powder (Sigma, St. Louis, MO) was serially diluted (0.2, 0.4, 0.6, 0.8, 1.0, 1.2, 1.4 ng/μL) in water (Sigma) to act as the inhibitory agent.

PCR Primers, Probe, and Assay Design

Analysis focused on a 134 bp region downstream from a dinucleotide microsatellite locus, GenBank® Accession L29229 (37). The Primer Express® Software (Version 2.0; Applied Biosystems, Foster City, CA) was used to design forward (5′-AACCCTC TCCATGTCTTTGTTCA), and reverse (5′-CTAGCAGACCTT ATGTTATAAAATTTCCAT) primers, as well as a sequence-specific TaqMan®-MGB (minor groove binder) probe (6FAM-TT ACGTTGCTGGACTATAC-MGBNFQ). A GenBank® BLAST search for short nearly exact matches revealed no significant database alignments with either primer or the MGB probe other than the region of interest in the porcine genome.

Amplification assays contained 12.5 μL TaqMan® Universal PCR Master Mix (1 × final; Applied Biosystems), 0.45 μL each primer (900 nM), 0.63 μL MGB probe (250 nM), 2.5 μL template DNA, 1 μL tannic acid solution, and 7.47 μL sterile water (Sigma) with a total volume of 25 μL. All possible combinations of template DNA and tannic acid were amplified in triplicate ($n = 264$). Amplifications containing template DNA but no tannic acid as well as no-template reactions were included throughout this experiment as positive and negative controls.

Real-time PCR was performed using the ABI PRISM® 7000 Sequence Detection System (Applied Biosystems). Following enzyme activation at 95°C for 10 min, the samples were amplified for 50 cycles at 95°C for 15 sec and 68°C for 1 min.

The amplicon selected for this study shares several attributes with the STR loci used in human forensic DNA testing. According to Butler et al. (38), the loci amplified by the Promega Powerplex® 16 system have an average primer length of 24.0 ± 4.3 bases (compared with 26.5 bases for L29229), an average %GC of 42.9 ± 8.5% (compared with 43.5% for L29229), and an average annealing temperature of 67.4 ± 1.9°C (compared with 68°C for L29229). Furthermore, the L29229 amplicon is within the size range of the forensic STR loci.

Data Analysis: Template DNA Quantitation, Amplification Efficiencies, and Outlier Detection

The ABI Prism 7000 Sequence Detection Software (Version 1.0; Applied Biosystems) generated fluorescence data that were used to develop standard quantitation curves (Fig. 1*b*) and to calculate individual reaction amplification efficiencies. The baseline was established between cycle 6 and cycle 15. The threshold was then set at 0.2, a fluorescence value above the background fluorescence noise in the steepest (i.e., maximal slope) portion of the log ΔR_n versus cycle number plot (Fig. 1*a*). Standard curves constructed from the clean standards were used to assess the effects of tannic acid on quantitation estimates.

Amplification efficiencies were then calculated using the Liu and Saint, and the LinRegPCR methods. For the Liu and Saint calculation, fluorescence values at the CT were used as the first arbitrary point ($\Delta R_{n,A}$). The second point ($\Delta R_{n,B}$) was set four cycles later at CT+4. In order to determine the optimal adjustment strategy for detecting problematic samples, efficiencies were also calculated by anchoring $\Delta R_{n,A}$ at CT − 3, CT − 2, CT − 1, CT+1, CT+2, and CT+3, and likewise adjusting $\Delta R_{n,B}$ to maintain a four-cycle distance from $\Delta R_{n,A}$.

The LinRegPCR software uses predefined criteria to select fluorescence values within the exponential phase of the real-time PCR plot. Ramakers et al. (30) recommend visual inspection of the amplification curves to identify anomalous samples that require window-of-linearity adjustments or exclusion from analysis. Table 1 presents the automated selection criteria along with the window-of-linearity adjustments evaluated in this study. The first adjustment minimizes data manipulation by re-configuring the window of linearity only when amplification efficiencies exceed the theoretical maximum value of 2.0. The second adjustment also requires subjective evaluation; however, the focus shifts from maximizing efficiency to including CT in the window of linearity. The remaining adjustments further minimize subjectivity by anchoring the window at CT − 1, CT, or CT+1. When possible, amplification efficiencies were calculated over a four-cycle interval. Using less than four data points increases the effects of stochastic fluctuations on the calculation, whereas more data points increases, the possibility that fluorescence values outside the exponential phase will affect the efficiency estimate. Including a consistent number of data points allows for direct comparison between the Liu and Saint and the LinRegPCR methods.

TABLE 1—*LinRegPCR efficiency calculation and adjustment criteria.*

	Adjustment Criteria (in order of priority)
Unadjusted (Raw LinRegPCR output)	4–6 data points Highest R^2 value Slope closest to maximum
Adjustment 1	4–6 data points $R^2 > 0.99$ Efficiency closest to maximum without exceeding $E = 2.0$
Adjustment 2	Ideally 4 data points, but allowed maximum of 6 Window-of-linearity encompasses CT Highest R^2 value
Adjustment 3	4 data points Window-of-linearity anchored at CT − 1
Adjustment 4	4 data points Window-of-linearity anchored at CT
Adjustment 5	4 data points Window-of-linearity anchored at CT+1

CT, threshold cycle.

Kinetic outlier detection (KOD) boundaries and prediction boundaries (PB) were used to identify template samples with depressed efficiency values. KOD utilizes the estimated sample variance in efficiency calculated for the clean standards to construct an interval estimate (39). This method is capable of flagging reactions with amplification efficiencies significantly greater or lesser than clean standards. However, the two-tailed approach cannot discriminate between the high or low outliers. As we assume that inhibitors suppress efficiency, the equation is modified to identify samples with significantly diminished efficiency values. Therefore, an unknown sample is flagged as an outlier if

$$P^* = \Phi\left(\frac{e_i - \mu_{\text{std}}}{\sigma}\right) < 0.05$$

where Φ is the cumulative distribution function of the standard normal curve, e_i is the efficiency of the unknown sample, μ_{std} is the mean efficiency of the standard samples, and σ is the standard deviation of the standard samples.

The one-tailed KOD method is compared with a one-tailed 95% prediction boundary:

$$y - t_{\alpha=0.05} s_e \sqrt{1 + \frac{1}{n} + \frac{(x - \bar{x})^2}{S_{xx}}}$$

where y is the predicted efficiency at a given CT value (x) based on linear regression, t is the t-distribution value at $\alpha = 0.05$ with $n - 2$ degrees of freedom, s_e is the sample standard error of estimate for the regression of efficiency (y) on CT (x), $\bar{x}$ is the mean CT value for the clean standards, S_{xx} is the sum of squares of CT, and n is the sample size.

Results

Tannic Acid Effects on Real-Time PCR Quantitation

Tannins and other oligomeric compounds with free phenolic groups (e.g., humic acids) oxidize to form quinones, which covalently bond to and inactivate *Taq* DNA polymerase (35). As a result, amplification efficiencies are reduced. Inhibition severity is directly related to the amount of tannins present, with complete inhibition of the TaqMan® real-time PCR assay occurring at concentrations greater than 1.4 ng per 25 µL reaction. However, tannin concentrations below 1.4 ng per 25 µL reaction will also impede amplification and confound real-time quantitation estimates.

A real-time amplification plot of the 50,000 pg DNA assays with increasing concentrations of tannic acid demonstrates the effects of PCR inhibition on amplification efficiency and accumulated fluorescence (Fig. 2*a*). As inhibitor concentrations increase,

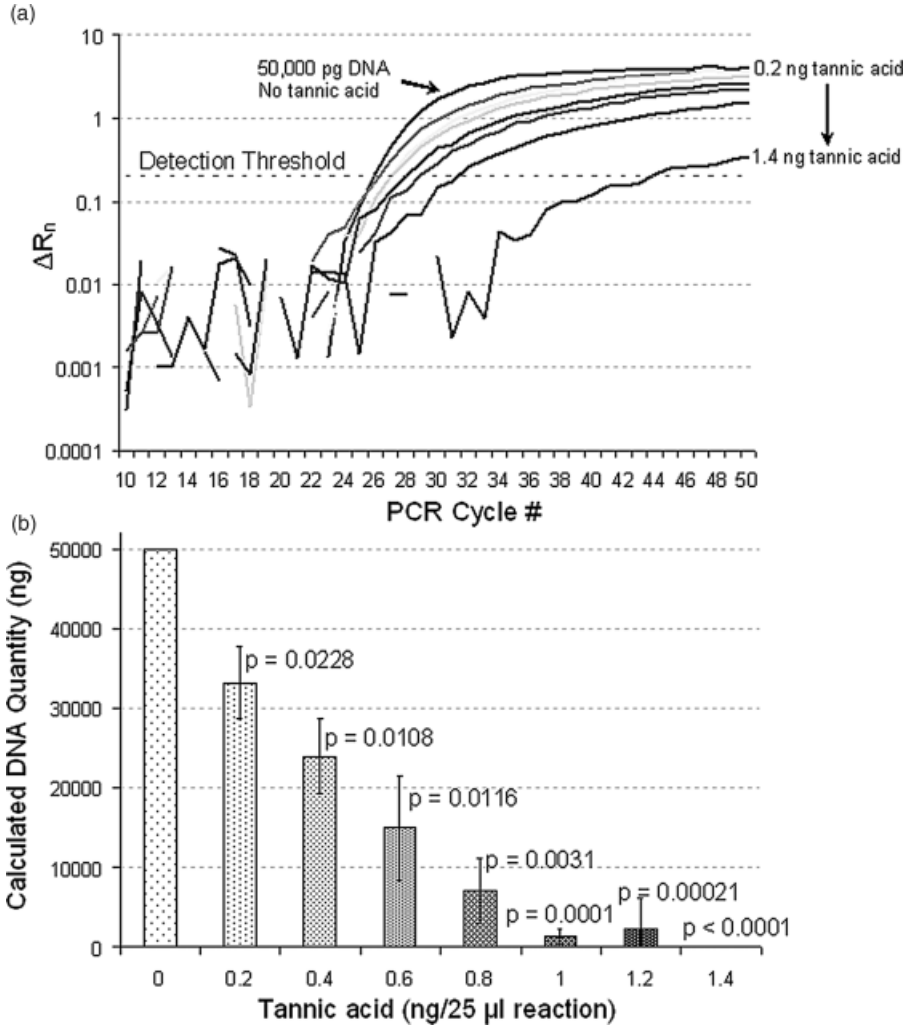

FIG. 2—*(a) Semi-log real-time PCR amplification plot of 50,000 pg template DNA samples with increasing concentrations of tannic acid (0.2–1.4 ng/25 µL reaction). As tannic acid concentrations increase, reactions cross the detection threshold at later cycles and reaction curve slopes decrease. (b) Delayed crossing of the detection threshold results in significantly depressed quantitation estimates (± 1 SD) for the tainted samples (one-sample t-test).*

reactions cross the detection threshold at later cycles and the exponential phase slopes decrease. Suppressed amplification efficiencies also have a negative effect on the linear phase and as a result, tannin-spiked samples approach lower plateau fluorescence values at the end of the reaction sequence. The ABI sequence detection software calculates template DNA concentration assuming equal amplification efficiencies between the standards and test samples. Consequently, quantitation estimates are significantly lower for all tannin-spiked samples compared with the expected value of 50,000 pg (Fig. 2*b*).

Identifying suspect reactions by visual inspection of the amplification plot is possible if quantitation estimates are substantially lower than expected, as when fresh tissue template DNA samples are contaminated by PCR inhibitors. In forensic contexts, this subjective approach is often not feasible as tissue samples are degraded or otherwise compromised due to environmental exposure. It is therefore necessary to select an appropriate efficiency calculation and outlier identification strategy in order to maximize the inhibitor detection potential of the real-time PCR system.

Method Adjustments and Concordance

The Liu and Saint equation is used to calculate efficiency at several anchoring points within three cycles of the threshold (CT) (Fig. 3). Adjusting the anchoring point to include fewer background fluorescence values decreases stochastic variation in the efficiency estimates, which results in less overlap between mean efficiencies for each level of tannic acid treatment. As the anchoring point moves further along the reaction, more plateau-phase data points are included in the calculation and efficiency estimates decrease. Anchoring the calculation at higher cycles mitigates stochastic effects, but the decrease in amplification efficiency results in a substantial overlap between the tannic acid treatments. Increasing concentrations of tannic acid will have a significant influence on amplification efficiency regardless of the cycle used to anchor the calculation (ANOVA model p-values for each anchoring point <0.0001). However, Tukey–Kramer (T–K) pairwise comparisons between tannic acid treatments are not always significant (Fig. 3). Discriminating between clean samples and those contaminated with the lowest tannic acid concentrations (0.2 ng per 25 μL reaction) is only possible when the efficiency calculation is anchored between CT − 1 and CT+2 (T–K; $\alpha = 0.05$). In essence, minimizing stochastic and plateau effects by anchoring the efficiency calculation around CT will maximize discrimination capabilities.

Similar results are obtained using the LinRegPCR method (Fig. 4). As a consequence of maximizing slope, the LinRegPCR software anchors the window of linearity at an average of CT–2.38 cycles. As observed with the Liu and Saint adjustments, including data points below CT increases the potential influence of stochastic fluctuations on the efficiency estimate. Consequently, unadjusted LinRegPCR efficiency estimates are highly variable with substantial overlap between tannic acid treatments. Most problematic is an inability to distinguish the clean reactions from those treated with 0.2 ng of tannic acid (T−K; $\alpha = 0.05$). Adjusting the LinRegPCR method to maintain high R^2 and slope values without exceeding the theoretical efficiency maximum shifts the window of linearity anchoring point to an average of CT–1.44 cycles. Arranging the window to include CT (adjustment 2) decreases variation in the efficiency estimate and increases discrimination between treatments. Adjustment 2 also allows discrimination between clean and tainted samples. The remaining adjustments shift focus away from maximizing efficiency and remove subjectivity by anchoring the window within one cycle of the threshold. These adjustments perform as well as adjustment 2, with the only overlaps in mean efficiency noted at high tannic acid concentrations, in essence, ensuring that the window of linearity includes CT improves discrimination between clean and tannic acid-contaminated samples.

Unfavorable properties such as systematic deviations in the efficiency estimates can be revealed by an analysis of method concordance. As expected, the highest coefficients of determination between the Liu and Saint calculations and the anchored LinRegPCR adjustments are observed among CT+1 and adjustment

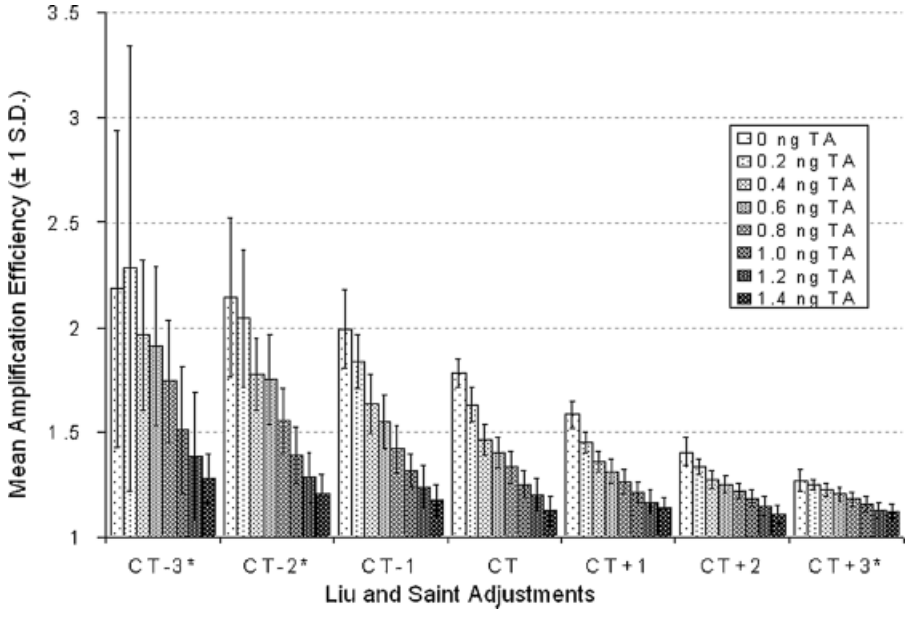

FIG. 3—*Mean amplification efficiencies for each tannic acid (TA) treatment group calculated using the Liu and Saint equation (± 1 SD). As the anchoring cycle moves out of the background real-time PCR detection phase, stochastic effects decrease. Also, the mean efficiencies decrease as the adjustments include more linear phase data points.* *Non-significant differences in amplification efficiency between the clean assays and the 0.2 ng TA assays (Tukey–Kramer pairwise comparisons, $\alpha = 0.05$).

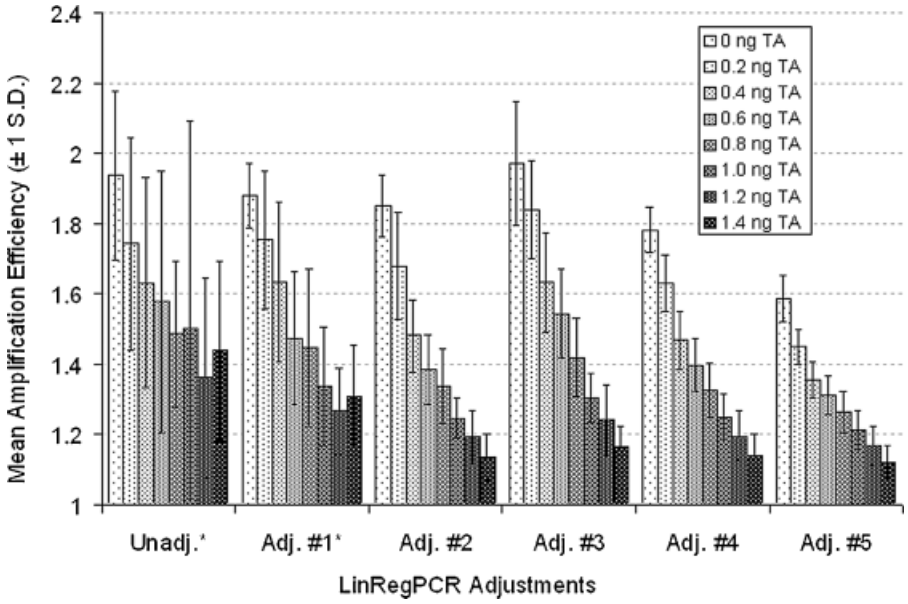

FIG. 4—*Mean amplification efficiencies for each tannic acid (TA) treatment group calculated using the LinRegPCR method (± 1 SD). Stochastic effects are reduced as emphasis shifts from maximizing efficiency (unadj. & adj. #1) to anchoring in relation to CT (adj. #2–5). *Non-significant differences in amplification efficiency between the clean assays and the 0.2 ng TA assays (Tukey–Kramer pairwise comparisons, $\alpha = 0.05$).*

5 (Table 2). These results underscore the fact that anchoring at CT+1 (i.e., adjustment 5) minimizes both the stochastic errors in measurement associated with a lower threshold and the loss of resolution, or "flattening" of efficiency estimates seen at higher thresholds (Figs. 3 and 4). Furthermore, there is a general trend toward overestimating efficiency when unanchored LinRegPCR estimates are regressed against the Liu and Saint values (data not shown). Overestimation is expected in these cases, as the LinRegPCR method emphasizes maximizing the efficiency estimate. This relative overestimation is minimized when anchored estimates are evaluated. Concordance analysis suggests that the two methods produce similar results, provided that calculations are anchored at the same cycle.

Efficiency Outlier Detection

Analysis of mean amplification efficiencies provides information on treatment-specific effects such as sample quality variation between extraction methods or tissues. However, identifying individual efficiency outliers requires analysis of the relationship between amplification efficiencies and CT values (Fig. 5). Outlier detection is predicated on the assumption that clean template DNA samples have consistent amplification efficiencies over a broad concentration range. The DNA standards used in this study follow this trend, showing no significant relationship between efficiency and CT (ANOVA, $F = 0.893$, $p = 0.3521$). Although not significant, a negative trend is apparent (linear regression slope = -0.0031), which is consistent with the detrimental impact the prolonged thermocycling has on *Taq* DNA polymerase activity (40). The decline in *Taq* activity manifests as a decline in efficiency when template DNA concentrations are low and real-time PCR product accumulation and fluorescence detection is delayed. However, the robust nature of the TaqMan® DNA polymerase, which has a half-life of 40 min at 95°C (41), minimizes efficiency decay.

As tannic acid concentrations increase, amplification efficiencies decline and CT values increase (Fig. 5). However, substantial overlap with clean standards exists at low inhibitor concentrations. KOD and PB are constructed to identify samples with significantly deviating efficiency estimates. PB relax the assumption of equal variance in efficiency over a broad range of CT values implicit in the KOD method. In other words, the prediction boundary should be sensitive to real-time PCR dynamic range limitations, which could influence reaction efficiencies at extreme template concentrations. Even though both methods are equally conservative ($\alpha = 0.05$), the 95% prediction boundary is assumed to be less sensitive at extreme CT values due to relaxation of the equal variance assumption. As a result, a 0.4 ng reaction flagged as an outlier by the KOD method is considered within the prediction boundary (Fig. 5). However, the greatest potential for overlap between clean and tainted assays exists at low tannic acid concentrations, where the outlier detection boundaries are comparable. Assays treated with high concentrations of tannic acid fall well below either detection boundary, so the increasing discrepancy between the two boundaries at high CT values is not a factor. Logistic regression analysis confirms that the performance differences between the outlier detection methods are negligible irrespective of the efficiency calculation and adjustment method utilized (Liu and Saint: $\chi^2 = 3.10$, $p = 0.0781$; LinRegPCR: $\chi^2 = 1.20$, $p = 0.2738$).

TABLE 2—*Coefficients of determination for all pairwise method comparisons.*

	Unadj	Adj 1	Adj 2	Adj 3	Adj 4	Adj 5
CT − 3	0.131	0.219	0.210	0.361	0.293	0.235
CT − 2	0.191	0.425	0.626	0.793	0.721	0.633
CT − 1	0.218	0.549	0.770	0.986	0.909	0.853
CT	0.205	0.583	0.869	0.916	0.990	0.920
CT+1	0.191	0.550	0.853	0.844	0.944	**0.992**
CT+2	0.156	0.479	0.747	0.774	0.880	0.938
CT+3	0.123	0.457	0.647	0.672	0.761	0.828

High R^2 values are observed for the anchored adjustments (adj. 3–5), with the highest value achieved between adjustment 5 and the CT+1 methods (bold).

CT, threshold cycle.

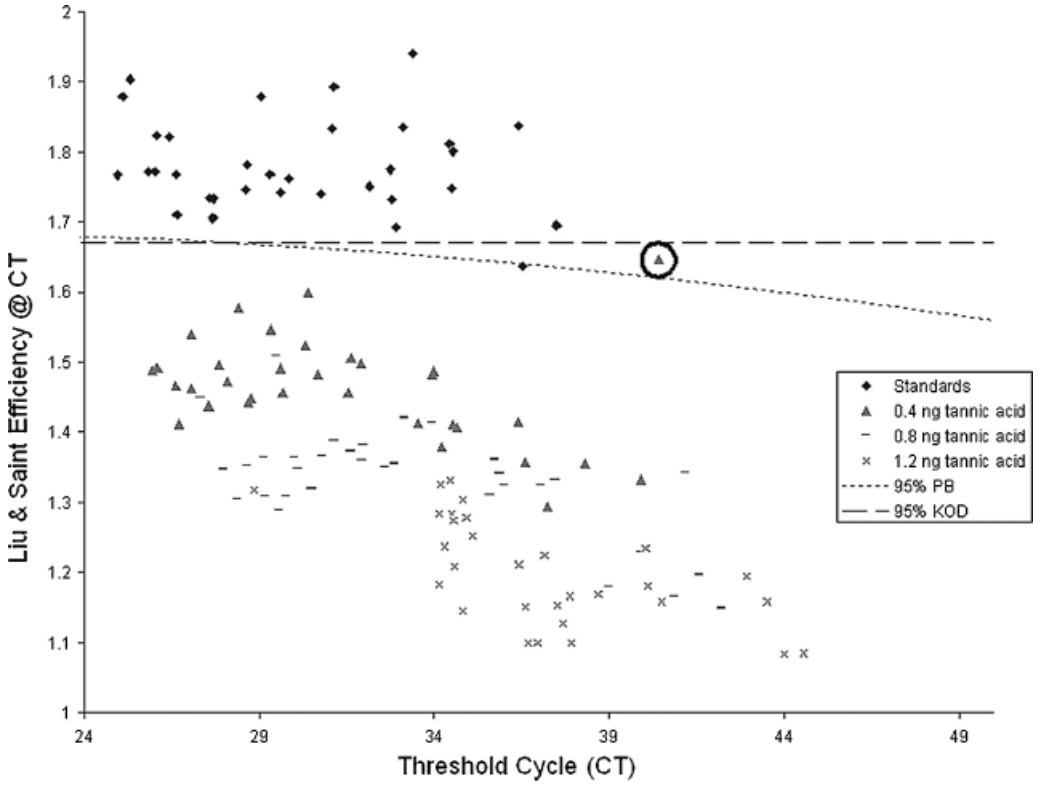

FIG. 5—*Relationship between amplification efficiencies calculated using the Liu and Saint method anchored at CT to the cycle at which the reactions cross the detection threshold (CT). The 95% kinetic outlier detection (KOD) and prediction boundaries (PB) are also depicted. As CT increases, the PB becomes more conservative and fails to detect a sample spiked with 0.4 ng of tannic acid (circled). The 0.2, 0.6, 1.0, and 1.4 ng tannic acid treatment groups are not depicted to aid visualization.*

Inhibitor Detection Power Analysis

While there are no significant performance differences between the KOD and PB outlier identification methods, selecting an appropriate efficiency calculation adjustment enhances the ability to discriminate between clean samples and those contaminated by even minor quantities of PCR inhibitors (Figs. 6 and 7). Based on logistic regression analysis, adjustment has a significant effect on outlier detection for the Liu and Saint method ($\chi^2 = 777.54$, $p < 0.0001$) as well as the LinRegPCR approach ($\chi^2 = 258.33$, $p < 0.0001$).

Anchoring the Liu and Saint calculation at CT or CT+1 provides maximum outlier detection power at the 0.2, 0.4, and 0.6 ng tannic acid treatments (Figs. 6*a* and *b*). Higher tannic acid concentrations severely depress amplification efficiencies, enabling outlier discrimination using less sensitive methods. Nevertheless, identifying tainted samples was not possible with the CT − 3-anchored calculation even at the highest tannic acid concentrations. Similar results are obtained with the KOD and PB methods for the CT and CT+1 adjustments. However, the KOD method allows greater discrimination when the anchoring point deviates from the optimal setting (Figs. 6*a* and *b*).

The LinRegPCR efficiency calculation results are comparable to the Liu and Saint analyses. Optimal detection is achieved when the window of linearity includes CT (adjustment 2), or is anchored at CT (adjustment 4) or CT+1 (adjustment 5) (Figs. 7*a* and *b*). Outlier detection sensitivity declines significantly when the window is adjusted to maximize the efficiency estimate (adjustment 1). Similarly, anchoring the adjustment at CT-1 (adjustment 3) is ineffective; however, this approach is more powerful than the efficiency maximization adjustment in all cases, except for the 0.2 ng treatment group. As demonstrated by Fig. 4, the unadjusted data have the worst efficiency estimation properties, which result in poor outlier detection performance. As with the Liu and Saint calculations, the KOD method is more sensitive to non-optimal window-of-linearity adjustments, especially with the unadjusted data (Figs. 7*a* and *b*).

As the anchoring point moves away from CT, discriminating between standards and contaminated samples becomes more challenging. When more baseline data points are included, the variance of the standards increases, which results in broader KOD and PB estimates. Consequently, fewer tainted samples fall outside the boundaries, even at the highest tannic acid concentrations. As the anchoring point moves to include more plateau-phase values (i.e., above CT+1), efficiency estimates are depressed, thus confounding the efficiency estimates. Both efficiency calculation methods allow for sensitive detection within a narrow adjustment window centered at CT. It is therefore imperative to adjust the selected method accordingly.

Discussion and Conclusions

Ramakers et al. (30) contend that the LinRegPCR method enables more reliable identification of efficiency outliers and greater confidence in template DNA quantitation estimates compared with the Liu and Saint approach. The results of this study do not support this assertion. Unadjusted LinRegPCR calculations consistently overestimate amplification efficiencies. Approximately 31% of the unadjusted calculations require adjustment to bring the efficiency estimates below the theoretical maximum ($E = 2.0$). Overestimation is a consequence of maximizing efficiency rather than ensuring that the window of linearity remains in

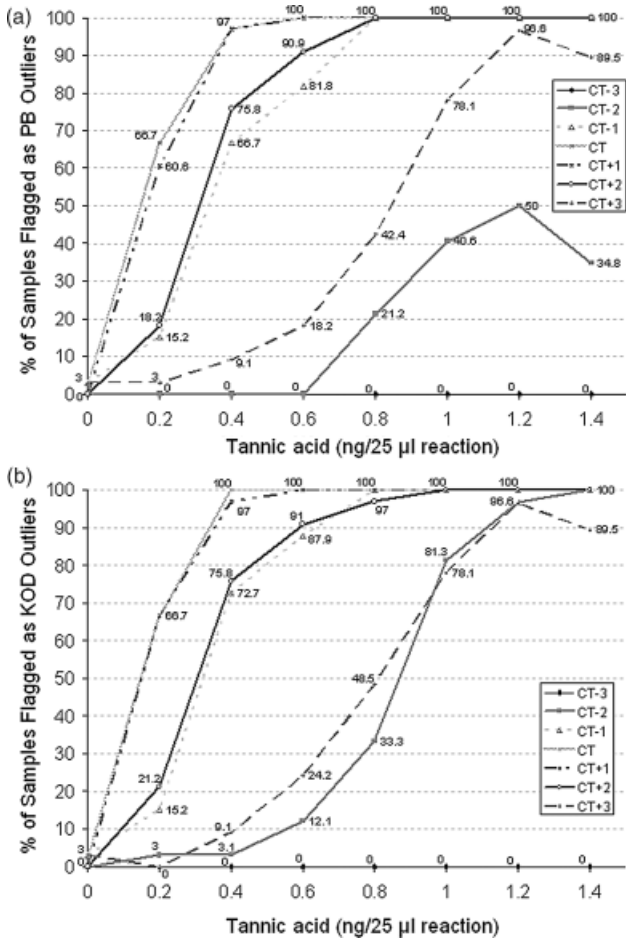

FIG. 6—*Liu and Saint inhibitor detection power analysis using the (a) 95% prediction boundary (PB) method, and (b) the kinetic outlier detection (KOD) method. Significant differences ($p < 0.05$) were noted between all adjustments and the CT and CT+1 anchored calculations for the 0.2–0.6 ng tannic acid treatments. Tannic acid treatments greater than 0.6 ng were not evaluated due to the certainty of being detected using either the PB or KOD method.*

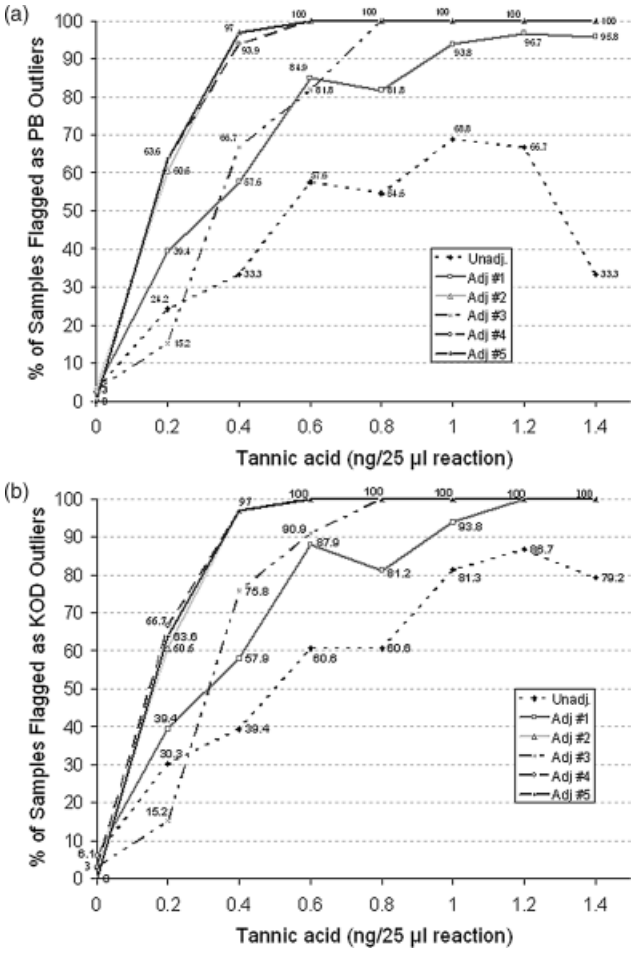

FIG. 7—*LinRegPCR inhibitor detection power analysis using the (a) 95% prediction boundary (PB) method, and (b) the kinetic outlier detection (KOD) method. Significant differences ($p < 0.05$) were noted between all adjustments and adjustments 2, 4, and 5 for the 0.2–0.6 ng tannic acid treatments. All assays with greater than 0.6 ng tannic acid were flagged as outliers by both methods and are not depicted in these figures.*

the exponential phase of the reaction. Theoretically, maximum amplification efficiency should occur during the exponential detection phase (42). However, stochastic processes in the background phase can lead to substantial elevation of the efficiency estimate, shifting the window to earlier cycles. If the linear regression approach is used, adjusting the window of linearity to encompass CT is essential to maximize outlier detection capabilities. Anchoring the window at CT or CT+1 minimizes analytic subjectivity and stochastic effects and as a result substantially improves method concordance.

While results are comparable, the Liu and Saint method requires no additional software and minimal manipulation of the ABI Prism SDS ΔR_n output. The LinRegPCR method utilizes software that is currently not capable of automating the adjustment process. Consequently, more substantial investments of time are necessary for LinRegPCR data analysis.

This study demonstrates that real-time PCR efficiency analysis is a sensitive inhibitor detection strategy when assays are contaminated with tannic acid. Tannic acid is a known PCR inhibitor (33–35,43) and is a recognized template DNA contaminant requiring specialized purification protocols (44). The mechanisms of PCR inhibition can be grouped into three categories based on the point of action during sample preparation and amplification (45). Inhibitors can interfere with cell lysis during DNA extraction (46,47); degrade or capture nucleic acids (48); or inhibit *Taq* DNA polymerase activity (47,49–52). While inhibitory mechanisms may vary, the outcome is a general reduction in amplification efficiency. Recent studies conducted by Green et al. (9) indirectly support this hypothesis. They present results demonstrating the negative relationship between increasing quantities of hematin on the slope of the real-time PCR amplification plots ((9), Fig. 4). These results are similar to those observed during the present study, which suggests that the proposed efficiency calculation methods can be utilized to detect the presence of other co-extracted PCR inhibitors.

However, a variety of substances with different properties or inhibitory mechanisms may not be identified as readily. For instance, the inhibitory effects of thermo-labile molecules may diminish as a function of repeated thermal cycling (53). During the early phases of the reaction, thermo-labile compounds may be potent inhibitors, with diminishing effects as the reaction progresses through its thermal cycling regime. As a result, threshold crossing will be delayed. Inhibitor degradation will eventually allow amplification efficiencies to recover and reactions to cross the detection threshold. In such situations, efficiency calculations will not be an effective detection strategy.

An alternative inhibitor detection strategy is to create a serial dilution of the suspect template and construct an intrinsic calibration curve from which efficiency can be estimated (25,54). Because of the exponential nature of PCR amplification, only a small number of template molecules are required to generate a PCR product. Thus, samples can often be diluted to a point where inhibitors are ineffective at preventing amplification of the remaining template DNA. As a result, diluted assays will cross the detection threshold earlier, decreasing the slope of the linear regression curve generated using the suspect sample dilution series. Efficiency is then calculated from the slope of the linear regression line:

$$E = 10^{-1/\text{slope}}$$

Low efficiency values suggest that dilution has reduced the effects of amplification inhibitors. While potentially useful, this alternative approach requires extensive sample manipulation and multiple PCR assays, increasing workloads and financial expenditures substantially. In addition, if template DNA concentrations are low, as is often the case in forensic contexts, dilution may result in template depletion and no amplicon production. Consequently, this method is of limited utility with challenging template samples.

Another important consideration is that the appropriate set of standards is used to construct the KOD and PB. In essence, the KOD and PB statistically evaluate differences between standards and samples. Amplification efficiencies can vary as a function of locus-specific properties such as amplicon size (55), so it is imperative that identical assays are used to develop comparative standards. Additionally, batch-specific variability in *Taq* DNA polymerase activity has been documented (56,57), which underscores the importance of using the same stock reagents for the standards and test samples.

This study empirically demonstrates that real-time PCR efficiency calculations can be used to evaluate template DNA quality and identify problematic samples prior to genotyping or DNA sequence analysis. The Liu and Saint and the LinRegPCR methods provide comparable efficiency estimates and similar outlier detection results. However, optimal performance is predicated on adjusting the calculations to minimize inclusion of baseline and linear-phase fluorescence values. Additionally, significant differences between the KOD and PB methods are not apparent when using the recommended adjustments. However, PB are less sensitive to non-optimal efficiency calculation adjustments. This discrepancy is consistent with relaxation of the equal variance assumption, which broadens the prediction boundary as data points move away from CT values in the center of the experimental range.

The objectives of this study are to present a basic computational method that will allow analysts to identify problematic samples with a defined level of statistical reliability. Internal Positive Controls (IPC) can also be used to detect the presence of PCR inhibitors (9). The IPC is particularly useful for detecting false-negative results; however, it cannot be used to ascertain a precise measure of inhibition severity when template samples are marginally compromised. Comparing the amplification efficiencies of clean standards with unknown samples is a statistically sound method that can be used in conjunction with IPC when amplifications are successful, but are compromised, producing erroneous quantitation results.

In summary, the Liu and Saint and LinRegPCR amplification efficiency calculations anchored at CT or CT+1, coupled with the KOD or PB outlier detection methods, provide a sensitive and statistically powerful strategy for identifying template DNA assays contaminated with PCR inhibitors. Based on ease of use, flexible assumptions, and maximum diagnostic power, we specifically recommend the Liu and Saint method anchored at CT+1. Utilizing these rigorous procedures to identify tainted samples offers a useful opportunity to consider inhibitor mitigation strategies prior to genotype or sequence analysis, facilitating sample processing.

Acknowledgments

The authors would like to thank Kenneth A.R. Kennedy, Charles Aquadro, Françoise Vermeylen, and members of the Aquadro and Clark Laboratories at Cornell University for insightful suggestions during all phases of this project. EJK would also like to thank Mark Leney and the anonymous reviewers for insightful comments during the manuscript revision process. This research was supported in part by grants to EJK by from the Forensic Sciences Foundation and the Cornell University Chapter of Sigma Xi. FAR was partially supported by the Center for Bioinformatics and Computational Biology, University of Maryland.

References

1. Handt O, Krings M, Ward RH, Paabo S. The retrieval of ancient human DNA sequences. Am J Hum Genet 1996;59:368–76.
2. Navidi W, Arnheim N, Waterman MS. A multiple-tubes approach for accurate genotyping of very small DNA samples by using PCR-statistical considerations. Am J Hum Genet 1992;50:347–59.
3. Takahashi M, Kato Y, Mukoyama H, Kanaya H, Kamiyama S. Evaluation of five polymorphic microsatellite markers for typing DNA from decomposed human tissues-correlation between the size of the alleles and that of the template DNA. Forensic Sci Int 1997;90:1–9.
4. Akane A, Matsubara K, Nakamura H, Takahashi S, Kimura K. Identification of the heme compound copurified with deoxyribonucleic acid (DNA) from bloodstains, a major inhibitor of polymerase chain reaction (PCR) amplification. J Forensic Sci 1994;39:362–72.
5. Wilson IG. Inhibition and facilitation of nucleic acid amplification. Appl Environ Microbiol 1997;63:3741–51.
6. Richard ML, Frappier RH, Newman JC. Developmental validation of a real-time quantitative PCR assay for automated quantification of human DNA. J Forensic Sci 2003;48:1041–6.
7. Walsh PS, Varlaro J, Reynolds R. A rapid chemiluminescent method for quantitation of human DNA. Nucleic Acids Res 1992;20:5061–5.
8. Waye JS, Presley LA, Budowle B, Shutler GG, Fourney RM. A simple and sensitive method for quantifying human genomic DNA in forensic specimen extracts. Biotechniques 1989;7:852–5.
9. Green RL, Roinestad IC, Boland C, Hennessy LK. Developmental validation of the Quantifiler™ real-time PCR kits for the quantification of human nuclear DNA samples. J Forensic Sci 2005;50:809–25.
10. Higuchi R, Dollinger G, Walsh PS, Griffith R. Simultaneous amplification and detection of specific DNA-sequences. Bio-technol 1992;10:413–7.
11. Higuchi R, Fockler C, Dollinger G, Watson R. Kinetic PCR analysis—real-time monitoring of DNA amplification reactions. Bio-technol 1993; 11:1026–30.
12. Alonso A, Martín P, Albarrán C, García P, García O, Fernández de Simón L, et al. Real-time PCR designs to estimate nuclear and mitochondrial DNA copy number in forensic and ancient DNA studies. Forensic Sci Int 2004;139:141–9.
13. Andréasson H, Allen M. Rapid quantification and sex determination of forensic evidence materials. J Forensic Sci 2003;48:1280–7.
14. Nicklas JA, Buel E. Development of an *Alu*-based, real-time PCR method for quantitation of human DNA in forensic samples. J Forensic Sci 2003;48:936–44.
15. Alonso A, Martín P, Albarrán C, García P, Primorac D, García O, et al. Specific quantification of human genomes from low copy number DNA samples in forensic and ancient DNA studies. Croat Med J 2003;44: 273–80.
16. Wetton JH, Tsang CSF, Roney CA, Spriggs AC. An extremely sensitive species-specific ARMS PCR test for the presence of tiger bone DNA. Forensic Sci Int 2002;126:137–44.
17. Ishida K, Zhu BL, Maeda H. Novel approach to quantitative reverse transcription PCR assay of mRNA component in autopsy material using the

TaqMan fluorogenic detection system: dynamics of pulmonary surfactant apoprotein A. Forensic Sci Int 2000;113:127–31.
18. von Wurmb-Schwark N, Higuchi R, Fenech AP, Elfstroem C, Meissner C, Oehmichen M, et al. Quantification of human mitochondrial DNA in a real time PCR. Forensic Sci Int 2002;126:34–9.
19. Heid CA, Stevens J, Livak KJ, Williams PM. Real time quantitative PCR. Genome Res 1996;6:986–94.
20. Morrison TB, Weis JJ, Wittwer CT. Quantification of low-copy transcripts by continuous SYBR® green I monitoring during amplification. Biotechniques 1998;24:954.
21. Wittwer CT, Herrmann MG, Moss AA, Rasmussen RP. Continuous fluorescence monitoring of rapid cycle DNA amplification. Biotechniques 1997;22:130–8.
22. Holland PM, Abramson RD, Watson R, Gelfand DH. Detection of specific polymerase chain reaction product by utilizing the $5' \rightarrow 3'$ exonuclease activity of *Thermus aquaticus* DNA polymerase. Proc Natl Acad Sci USA 1991;88:7276–80.
23. Gibson UEM, Heid CA, Williams PM. A novel method for real time quantitative RT-PCR. Genome Res 1996;6:995–1001.
24. Livak KJ, Flood SJ, Marmaro J, Giusti W, Deetz K. Oligonucleotides with fluorescent dyes at opposite ends provide a quenched probe system useful for detecting PCR product and nucleic acid hybridization. PCR Meth Appl 1995;4:357–62.
25. Ståhlberg A, Åman P, Ridell B, Mostad P, Kubista M. Quantitative real-time PCR method for detection of B-lymphocyte monoclonality by comparison of κ and λ immunoglobulin light chain expression. Clin Chem 2003;49:51–9.
26. Kains P. The PCR plateau phase–towards an understanding of its limitations. Biochim Biophys Acta 2000;1494:23–7.
27. Erlich H. PCR technology: principles and applications for DNA amplification. New York: Stockton Press, 1989.
28. Liu W, Saint DA. A new quantitative method of real time reverse transcription polymerase chain reaction assay based on simulation of polymerase chain reaction kinetics. Anal Biochem 2002;302:52–9.
29. Applied Biosystems. ABI Prism® 7000 sequence detection system [user guide]. Foster City, California: Applied Biosystems, 2002.
30. Ramakers C, Ruijter JM, Deprez RHL, Moorman AFM. Assumption-free analysis of quantitative real-time polymerase chain reaction (PCR) data. Neurosci Lett 2003;339:62–6.
31. Ruijter JM. LinRegPCR: analysis of real-time PCR data [computer program]. Version 7.5. Amsterdam, the Netherlands: Department of Anatomy and Embryology, Academic Medical Centre, 2004.
32. Bièche I, Laurendeau I, Tozlu S, Olivi M, Vidaud D, Lidereau R, et al. Quantitation of *MYC* gene expression in sporadic breast tumors with a real-time reverse transcription-PCR assay. Cancer Res 1999;59:2759–65.
33. Cooper A. Removal of colourings, inhibitors of PCR, and the carrier effect of PCR contamination from Ancient DNA samples. Ancient DNA Newsletter 1992;1:31–2.
34. Hummel S, Nordsiek G, Herrmann B. Improved efficiency in amplification of ancient DNA and its sequence analysis. Naturwissenschaften 1992;79:359–60.
35. Young C, Burghoff RL, Keim LG, Minak-Bernero V, Lute JR, Hinton SM. Polyvinylpyrrolidone-agarose gel electrophoresis purification of polymerase chain reaction-amplifiable DNA from soils. Appl Environ Microbiol 1993;59:1972–74.
36. Gallagher SR. Quantitation of DNA and RNA with absorption and fluorescence spectroscopy. In: Dracopoli NC, Haines JL, Korf BR, Morton CC, Seidman CE, Seidman JG, Smith DR, editors. Current protocols in human genetics. New York: John Wiley & Sons, 2003:A.3D.1–A.3D.8.
37. Robic A, Dalens M, Woloszyn N, Milan D, Riquet J, Gellin J. Isolation of 28 new porcine microsatellites revealing polymorphism. Mamm Genome 1994;5:580–3.
38. Butler JM, Devaney JM, Marino MA, Vallone PM. Comparison of primer sequences used in commercial STR kits. In: Proceedings of the American Academy of Forensic Sciences; 2001 February 19–26; Seattle. Colorado Springs, CO: American Academy of Forensic Sciences, 2001.
39. Bar T, Ståhlberg A, Muszta A, Kubista M. Kinetic outlier detection (KOD) in real-time PCR. Nucleic Acids Res 2003;31:e105.
40. Gelfand DH, White TJ Thermostable DNA polymerases. In: Innis MA, Gelfand DH, Snisky JJ, White TJ, editors. PCR protocols: a guide to methods and applications. San Diego: Academic Press, 1990:129–41.
41. Applied Biosystems. TaqMan® Gold RT-PCR [kit protocol]. Foster City, California: Applied Biosystems, 2000.
42. Freeman WM, Walker SJ, Vrana KE. Quantitative RT-PCR: pitfalls and potential. Biotechniques 1999;26:112–25.
43. Kreader CA. Relief of amplification inhibition in PCR with bovine serum albumin or T4 gene 32 protein. Appl Environ Microbiol 1996;62:1102–6.
44. Qiagen. QIAGEN News [technical publication]. Valencia, California: QIAGEN Inc., 2000.
45. Wilson IG. Inhibition and facilitation of nucleic acid amplification. Appl Environ Microbiol 1997;63:3741–51.
46. Jacobsen CS, Rasmussen OF. Development and application of a new method to extract bacterial DNA from soil based on separation of bacteria from soil with cation-exchange resin. Appl Environ Microbiol 1992;58:2458–62.
47. Simon MC, Gray DI, Cook N. DNA extraction and PCR methods for the detection of *Listeria monocytogenes* in cold-smoked salmon. Appl Environ Microbiol 1996;62:822–24.
48. Lienert K, Fowler JCS. Analysis of mixed human/microbial DNA samples: a validation study of two PCR AMP-FLP typing methods. Biotechniques 1992;13:276–81.
49. Katcher HL, Schwartz I. A distinctive property of TTH DNA-polymerase—enzymatic amplification in the presence of phenol. Biotechniques 1994;16:84.
50. Powell HA, Gooding CM, Garrett SD, Lund BM, McKee RA. Proteinase inhibition of the detection of *Listeria monocytogenes* in milk using the polymerase chain reaction. Lett Appl Microbiol 1994;18:59–61.
51. Saulnier P, Andremont A. Detection of genes in feces by booster polymerase chain reaction. J Clin Microbiol 1992;30:2080–83.
52. Young C, Burghoff RL, Keim LG, Minak-Bernero V, Lute JR, Hinton SM. Polyvinylpyrrolidone-agarose gel electrophoresis purification of polymerase chain reaction-amplifiable DNA from soils. Appl Environ Microbiol 1993;59:1972–74.
53. Pruvost M, Geigl EM. Real-time quantitative PCR to assess the authenticity of ancient DNA amplification. J Archaeol Sci 2004;31:1191–7.
54. Mygind T, Birkelund S, Birkebæk NH, Østergaard L, Jensen JS, Christiansen G. Determination of PCR efficiency in chelex-100 purified clinical samples and comparison of real-time quantitative PCR and conventional PCR for detection of *Chlamydia pneumoniae*. BMC Microbiol 2002;2:17.
55. Meijernik J, Mandigeers C, van De Locht L, Tonnissen E, Goodsaid F, Raemaekers J. A novel method to compensate for different amplification efficiencies between patient DNA samples in quantitative real-time PCR. J Mol Diagn 2001;3:55–61.
56. Meunier JR, Grimont PAD. Factors affecting reproducibility of random amplified polymorphic DNA fingerprinting. Res Microbiol 1993;144:373–9.
57. Tyler KD, Wang G, Tyler SD, Johnson WM. Factors affecting reliability and reproducibility of amplification-based DNA fingerprinting of representative bacterial pathogens. J Clin Microbiol 1997;35:339–46.

Additional information and reprint requests:
Elias J. Kontanis, Ph.D.
Joint POW/MIA Accounting Command
Central Identification Laboratory
310 Worchester Avenue
Hickam AFB
HI 96853
E-mail: Elias.Kontanis@JPAC.PACOM.MIL